Journal of Medicinal Chemistry

Article

pubs.acs.org/jmc

Phthalazine Derivatives Containing Imidazole Rings Behave as Fe-SOD Inhibitors and Show Remarkable Anti-*T. cruzi* Activity in Immunodeficient-Mouse Mode of Infection

Manuel Sánchez-Moreno,*[,†] Fernando Gómez-Contreras,*[,‡] Pilar Navarro,*[,§] Clotilde Marín,[†] Francisco Olmo,[†] María J. R. Yunta,[‡] Ana María Sanz,[‡] María José Rosales,[†] Carmen Cano,[‡] and Lucrecia Campayo[‡]

[†]Departamento de Parasitología, Facultad de Ciencias, Universidad de Granada, E-18071 Granada, Spain

[‡]Departamento de Química Orgánica, Facultad de Química, Universidad Complutense, E-28040 Madrid, Spain

[§]Instituto de Química Médica, Centro de Química Orgánica M. Lora-Tamayo, CSIC, E-28006 Madrid, Spain

Supporting Information

ABSTRACT: A series of new phthalazine derivatives **1**−**4** containing imidazole rings were prepared. The monoalkylamino substituted derivatives **2** and **4** were more active in vitro against *T. cruzi* and less toxic against Vero cells than both their disubstituted analogues and the reference drug benznidazole. Compounds **2** and **4** highly inhibited the antioxidant parasite enzyme Fe-SOD, and molecular modeling suggested that they interact with the H-bonding system of the iron atom moiety. In vivo tests on the acute phase of Chagas disease gave parasitemia inhibition values twice those of benznidazole, and a remarkable decrease in the reactivation of parasitemia was found in the chronic phase for immunodeficient mice. Glucose metabolism studies showed that compounds **1**−**4** did not affect the succinate pathway but originated important changes in the excretion of pyruvate metabolites. The morphological alterations found in epimastigotes treated with **1**−**4** confirmed extensive cytoplasm damage and a high mortality rate of parasites.

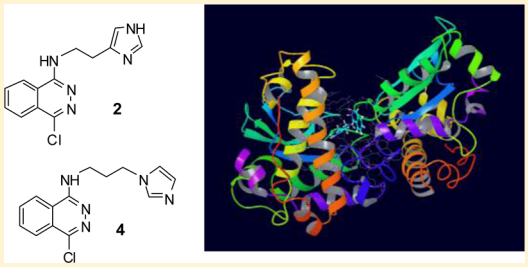

INTRODUCTION

The protozoan parasite *Trypanosoma cruzi* is responsible for Chagas disease, which is a potentially fatal considerable health problem in Latin America due to inadequate therapy and the lack of an effective vaccine.[1,2] Diverse factors, like increasing immigration, easy transmission via blood transfusion, pregnancy, and the compsumption of contaminated food, have contributed to the spread of the disease all over the world, and it is also progressively becoming a threat of major concern to health authorities in Europe and North America.[3,4] Many research groups have investigated the synthesis of molecules able to act efficiently on the amastigote forms of *T. cruzi*, but results obtained so far are unsatisfactory. The only two drugs currently used worldwide for the treatment of Chagas disease are the pentaheterocyclic derivatives nifurtimox and benznidazole. However, both drugs present significant side effects and limited efficacy, especially in the most lethal chronic phase of the disease. The most frequently prescribed is the imidazole derivative benznidazole (BZN), which is activated by nicotinamide adenine dinucleotide NADH-dependent trypanosomal reductases and forms reductive metabolites. Those metabolites supposedly cause a series of effects like DNA damage and inhibition of proteine synthesis, which breaks the respiratory chain in the amastigote forms of *T. cruzi*.[5,6] However, in adults, BZN generates a considerable number of adverse effects, mainly digestive (gastric upset, nausea, vomiting), hematologic (leukopenia, thrombocytopenia, agranulocytosis), dermatologic (erythema, dermatitis, Stevens−Johnson syndrome), and neurologic (dose-dependent polyineuropathies) alterations.[5,7] Furthermore, BZN originates reactive metabolites that interact with fetal components and has also shown tumorigenic or carcinogenic effects in some cases.[8] The effectiveness of BZN in the chronic phase is substantially lower than in the acute phase, and parasitological cure in the later chronic phase is only obtained in 10−20% of the patients.[9]

Another disturbing aspect of Chagas disease is the high reactivation ability of the parasitemia in immunocompromised individuals. It has been shown that apparently cured patients who had been further submitted to kidney or liver transplantation, diagnosed with acquired immunodeficiency syndrome (AIDS), or treated with anticancer chemotherapy experienced Chagas reactivation with a very aggressive clinical course leading to meningoencephalitis and/or acute myocarditis.[10−14] When patients with chronic chagasic cardiopathy undergo cardiac transplant, reactivation of the trypaniosomiasis occurs and treatment with benznidazole only leads to

Received: July 26, 2012
Published: October 8, 2012

dx.doi.org/10.1021/jm3011004 | *J. Med. Chem.* 2012, 55, 9900−9913

temporary remission, while *T. cruzi* infection persists.[15−17] From all of these facts it can be concluded that the design of new, less toxic drugs that are more effective against the chronic phase of Chagas disease and able to reduce reactivation in cases of immunodeficiency is urgently needed.

Antichagasic agent research mainly targets key metabolic biochemical pathways or crucial parasite-specific enzymes. Sterol metabolism, kinetoplast DNA sites, trypanothione reductase, cysteine proteinase, hypoxanthineguanine phosphoribosyltransferase, dihydrofolate reductase, and glyceraldehyde 3-phosphate dehydrogenase have fed the main lines of investigation in recent years.[18] Among the trypanosomatide-specific enzymes, we have focused our attention on iron superoxide dismutase (Fe-SOD) because it is not found in mammals and it plays an essential role in the defense of the parasite against oxidation. It has been shown that parasitic protozoan survival is closely related to the ability of that enzyme for evading toxic free radical damage originated by their host.[19] Because of the predominant role of the prostetic groups, interaction with the active sites containing the metal ion of Fe-SOD could be an efficient way of deactivating the antioxidant effect of the enzyme.

In relation to this matter, we have described in previous work new mono- and bis(alkylamino) derivatives of the benzo[*g*]-phthalazine system functionalized at the end of the alkylamine side chains with amino groups or heterocyclic units such as pyridine, pyrazole, or imidazole (Figure 1, general structures **I** and **II**).[20−22] Some of these compounds have shown very low toxicity against Vero cells and remarkable in vivo activity in mice infected with *T. cruzi* in both the acute and the chronic phases of the disease.[22] Activity results obtained for the chronic phase in parasitemia studies[22] are especially valuable because that stage of the disease is highly resistant to commonly used drugs. Furthermore, we found recently that those compounds that contained pyrazole or imidazole rings also present a significant in vitro activity against *Leishmania braziliensis* and *Leishmania donovani* species.[23] Structural features significantly influence the antiparasitic activity, since results obtained with the monoalkylamino substituted compounds **II** are much better than those of their type **I** disubstituted counterparts, as well as for those found for BZN. On the other hand, histopathological studies concluded that the monosubstituted derivatives containing imidazole rings are less toxic to mice than those with the pyrazole system.[22]

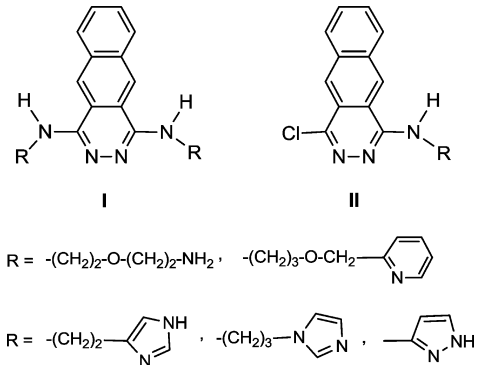

Figure 1. Benzo[*g*]phthalazine derivatives with potential antiparasitic activity.

Another remarkable result of our previous work was that both the imidazole and pyrazole derivatives were shown to be good inhibitors of the Fe-SOD antioxidant enzyme of the parasites, not only of *T. cruzi*[21] but also of *Leishmania* sp. species.[23] Furthermore, their inhibitory ability of human CuZn-SOD was negligible and, interestingly, the monoalkylaminosubstituted derivatives type **II** were also more powerful inhibitors of Fe-SOD than the disubstituted analogues. As commented before, Fe-SOD plays a key role in the defense of trypanosomatids against oxidation and it is not present in humans, so these findings are probably related to the antiparasitic activity obtained. Molecular modeling studies suggest that imidazole derivatives of type **II** can penetrate between the strands of the enzyme and locate an sp^2 imidazole nitrogen near one of the active sites[22] so that some kind of interaction with the environment of the iron atom could be responsible for the higher level of inhibition obtained in the assays performed.

On the basis of all of the results described above, we have prepared now structurally related imidazole derivatives in which the benzo[*g*]phthalazine moiety has been modified by the removal of one of the benzene rings (Figure 2, compounds **1**−**4**). That modification results in less bulky structures that could more easily approach the active sites of the enzyme. Removal of one aromatic ring should also reduce toxicity against the host and enhance solubility in aqueous media. This last feature makes synthesis and biological testing easier, but above all it has obvious pharmacological implications: an efficient trypanocidal agent must reach effective trypanocidal concentration levels in the blood plasma, biological fluids, and tissues of the host,[24] and its transport ability inside the parasite is also an essential feature.[5]

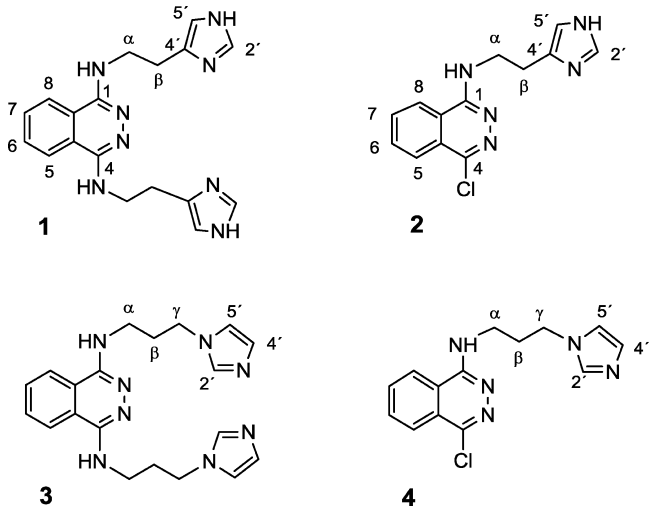

Figure 2. Imidazole-containing phthalazine derivatives tested against *T. cruzi* in this study.

In this work, the synthesis and characterization of compounds **1**−**4** is described along with an evaluation of their effectiveness as selective inhibitors of Fe-SOD in relation to human CuZn-SOD. Their in vitro antiparasitic activity and toxicity against Vero cells are tested and compared with values obtained for the reference drug BZN, and on the basis of the results obtained, their in vivo trypanosomicidal activity on female BALB/c mice is measured in both the acute and chronic phases. As commented above, one of the major unresolved problems caused by drugs currently in use is the lethality of *T. cruzi* infection in immunocompromised patients, as well as its

dx.doi.org/10.1021/jm3011004 | *J. Med. Chem.* 2012, 55, 9900−9913

failure to prevent the resurgence of the infection. The good activity results obtained with the benzo[*g*]phthalazine analogues in the chronic phase of the disease has prompted us to study, for the first time, the course of the infection in immunodeficient mice treated with *T. cruzi* and, thereafter, with compounds **1**−**4**. The effects of compounds **1**−**4** on the ultrastructure of *T. cruzi* are also studied by transmission electronic microscopy (TEM) experiments in order to confirm the type of damage caused to the parasite cells. Finally, an NMR analysis of the nature and percentage of the metabolites excreted is performed in order to gain some information about the inhibitory effects of these compounds on the glycolytic pathway, since this represents the prime energy source of the parasite.

RESULTS AND DISCUSSION

Chemistry. The preparation of compounds **1**−**4** was performed from 1,4-dichlorophthalazine according to the methodology shown in Scheme 1, following conditions related

Scheme 1. Preparation of the Imidazole-Containing Phthalazine Derivatives

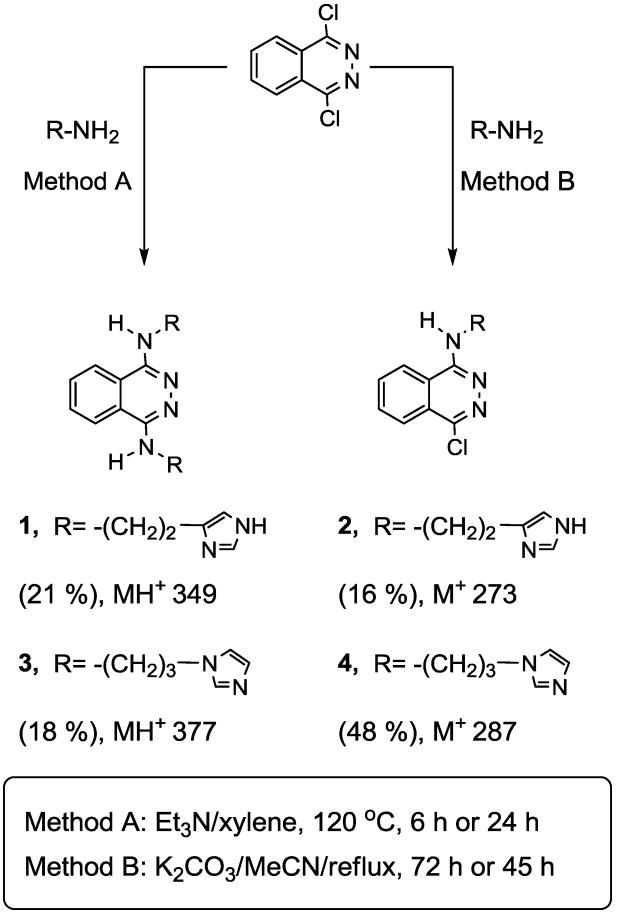

Method A: Et_3N/xylene, 120 °C, 6 h or 24 h
Method B: K_2CO_3/MeCN/reflux, 72 h or 45 h

to those previously established by our group for the synthesis of **I** and **II**[20−22] (Figure 1). The bis(alkylamino)substituted derivatives **1** and **3** were obtained with respective yields of 21% and 18% via simultaneous nucleophilic substitution at the C-1 and C-4 positions of the starting compound with 2-(imidazol-4-yl)ethylamine or 3-(imidazol-1-yl)propylamine under reflux of xylene for 6 or 24 h, using triethylamine as the chlorine acceptor (method A).[21]

Alternatively, the synthesis of the mono(alkylamino)-substituted compounds **2** and **4** was achieved using a different procedure in which the reaction was performed under reflux of acetonitrile over 72 or 45 h, and triethylamine was replaced by potassium carbonate (method B).[22] That modification usually leads to better yields of the monosubstituted compounds in relation to the disubstituted analogues, and in this case, yields of 16% and 48% were found for compounds **2** and **4**, respectively. Isolation of the compounds from the crude reaction mixtures was performed by column flash chromatography with a chloroform/methanol mixture of increasing polarity.

All of the newly synthesized compounds were unequivocally identified by their analytical, MS-ESI, IR, ^{1}H NMR, and ^{13}C NMR spectroscopic data, as shown in the Experimental Section. Scheme 1 displays the molecular ions obtained from the electrospray mass spectra, which agree in all cases with the proposed structures. For an accurate assignment of the ^{1}H and ^{13}C NMR spectra signals, registered in deuterated dimethylsulfoxide (DMSO-d_6), heteronuclear multiple quantum coherence (gHMQC) experiments were performed, and results were especially useful.

The mono- and bis(alkylamino) substitution products were easily differentiated in both ^{1}H and ^{13}C NMR spectra on the basis of signals corresponding to the ring atoms of the phthalazine system. Protons H-5 and H-8 (see numbering in Figure 2), which appeared as a unique singlet in the ^{1}H NMR spectra of **1** and **3**, lost their equivalence in the monosubstituted compounds **2** and **4**, with their chemical shifts differing by 0.28 and 0.18 ppm, respectively. The H-8 proton, close to the alkylamine chain, was deshielded with respect to the proton neighboring the chlorine atom (H-5). Accordingly, the carbon atom attached to the alkylamino substituent (C-1) was always deshielded with respect to the carbon neighboring the chlorine atom in the ^{13}C NMR spectra: carbons C-1 and C-4, identical in **1** and **3**, showed variations of 10.05 and 9.99 ppm in **2** and **4**, respectively. The carbon pairs C-4a/8a and C-5/8 also followed the same pattern, although the chemical shift differences were lower.

In Vitro Trypanosomicidal Evaluation. In order to get preliminary information, the in vitro activity of compounds **1**−**4** were evaluated against extracellular epimastigote and axenic amastigote forms of *T. cruzi* obtained from an SN3 strain isolated from Colombian *R. prolixus*, as described in the Experimental Section. More indicative data were found when the compounds were also tested on intracellular amastigotes, since extracellular forms are not the developed form of the parasite in vertebrate hosts. Therefore, Vero cells were infected with metacyclic forms of *T. cruzi* that were transformed into amastigotes within 1 day of infection and treated with **1**−**4**. Finally, the phthalazine derivatives were tested against blood trypomastigotes, since these forms of the parasite are responsible for the chronic phase of Chagas disease. Table 1 shows the IC_{50} values obtained after 72 h of exposure and at 1−100 μM when compounds **1**−**4** were assayed against the four parasite forms mentioned above. Values obtained for the reference drug BZN were included in all cases for comparison. Results obtained for all the *T. cruzi* forms studied were very homogeneous. As happened with the benzo[*g*]phthalazine analogues, the monoalkylamino substituted compounds **2** and **4** were always more active than their bis(alkylamino) substituted counterparts **1** and **3**, so the structural influences upon activity proposed in previous studies[21,22] were confirmed. Differences

dx.doi.org/10.1021/jm3011004 | *J. Med. Chem.* 2012, 55, 9900−9913

Table 1. In Vitro Activity and Toxicity Found for the Phthalazine Derivatives 1−4 against Extra- and Intracellular Forms of *T. cruzi*[a]

	activity, IC_{50} (μM)[b]				
compd	epimastigote form	axenic amastigote form	intracellular amastigote form	blood trypomastigote form	toxicity Vero cells IC_{50} (μM)[c]
BZN	15.9 ± 1.1	18.9 ± 1.5	23.3 ± 4.6	16.4 ± 3.2	13.6 ± 0.9
1	13.0 ± 0.8	15.2 ± 1.2	18.1 ± 1.5	22.5 ± 3.7	323.6 ± 14.3
2	8.7 ± 1.1	10.1 ± 0.7	9.4 ± 1.2	9.2 ± 0.7	427.3 ± 17.3
3	17.4 ± 2.0	12.4 ± 0.9	16.6 ± 0.8	16.9 ± 4.0	301.5 ± 11.8
4	8.8 ± 0.5	10.6 ± 0.4	8.9 ± 0.6	10.2 ± 1.2	436.7 ± 20.1

[a]The results are averages of three separate determinations. [b]IC_{50} = the concentration required to give 50% inhibition, calculated by linear regression analysis from the K_c values at concentrations employed (1, 10, 25, 50, and 100 μM). [c]Against Vero cells after 72 h of culture.

in activity between **2** and **4** were not significant and remained below the experimental error in all cases. When comparing with the reference drug, it was evident that the monosubstituted compounds were substantially more effective than BZN in the four cases considered.

The cytotoxicity of compounds **1−4** was evaluated using mammalian Vero cells as the cellular model (Table 1). Toxicity data were highly interesting because they confirmed that all of the phthalazine derivatives were substantially less cytotoxic than the corresponding compounds containing the benzo[*g*]-phthalazine moiety, in accordance with the previously outlined hypothesis that the elimination of one of the benzene rings should lead to lower toxicity levels. For instance, the monosubstituted compounds **2** and **4** showed IC_{50} values of 427.3 and 436.7 μM, whereas values of 213.0 and 145.8 μM had been found for their respective benzo[*g*]phthlazine analogues.[21] On the other hand, the most active monosubstituted compounds **2** and **4** were less toxic than **1** and **3**, and all of them were much less toxic than BZN, for which an IC_{50} value as small as 13.6 μM was obtained.

From the in vitro data shown above, the more informative selectivity index (SI) values were calculated and are shown in Table 2. When the number of times that the SI of each compound exceeded the SI of BZN (in parentheses) were calculated, very good results were found for the monosubstituted derivatives: the SI values of **2** and **4** exceeded those of BZN by 61-, 60-, 75-, and 58-fold and by 62-, 59-, 82-, and 53-fold, respectively. The best comparative results (75- and 82-fold) were obtained when the compounds were tested against the most significant intracellular amastigote forms. These data support the convenience of carrying out in vivo assays in order to confirm the apparent advantages found in vitro for compounds **2** and **4** with respect to BZN.

Table 2. Selectivity Index Found for the Phthalazine Derivatives 1−4 agaist Extra- and Intracellular Forms of *T. cruzi*

	SI[a]			
compd	epimastigote form	axenic amastigote form	intracellular amastigote form	blood trypomastigote form
BZN	0.8	0.7	0.6	0.8
1	24.9 (31)	21.3 (30)	17.9 (30)	14.4 (18)
2	49.1 (61)	42.3 (60)	45.5 (75)	46.5 (58)
3	17.3 (22)	24.2 (34)	18.2 (30)	17.8 (22)
4	49.6 (62)	41.2(59)	49.1 (82)	42.8 (53)

[a]Selectivity index = (IC_{50} of cell Vero)/(IC_{50} of extracellular and intracellular forms of parasite). In parentheses are the number of times that a compound SI exceeds the reference drug SI.

Going one step further in the activity study, the effect of the four compounds on the infectivity, intracellular replication of amastigotes, and further transformation of these in trypomastigotes was determined. For these assays, the IC_{25} of each product was used as the test concentration, with BZN as the reference drug. Vero cells were cultured for 2 days and then infected with epimastigote forms in the stationary phase. The parasites invaded the cells and underwent morphological conversion to amastigotes within 2 days of infection. On day 10, the rate of host cell infection reached its maximum in the control experiment (Figure 3A). When the imidazole derivatives **1−4** were added to the infected Vero cells, the infection rate significantly decreased with respect to the control for all of the compounds tested, leading to inhibition values varying from 51.5% to 83.3%. The four compounds were more effective than BZN, which showed a 39.4% inhibition, and the monosubstituted derivatives **2** and **4** were by far the most efficient of all (80.3% and 83.3% inhibition, respectively).

On the other hand, data on the mean number of amastigotes per infected Vero cell (Figure 3B) led to similar but even more compelling conclusions, since the four compounds were found to be much more effective than BZN, which only achieved 12.5% inhibition on day 10. Concerning the mean number of trypomastigotes detected (Figure 3C), although differences with BZN were less significant on the whole, inhibition values as high as 85.1% and 73.9% were found for the monosubstituted derivatives **2** and **4**, respectively, doubling the inhibition obtained for BZN (41.6%). Finally, compound **2** appeared to be a better inhibitor of parasitemia than **4** in the three cases (83.9%, 62.9%, and 85.1% against 80.3%, 55.8%, and 73.9%, respectively). The same thing happened with the couple **1** and **3**, where compound **1** was always more active than **3**. We think that the presence of an NH group in the imidazole rings of **1** and **2** could be related to the differences found with respect to **3** and **4**.

Inhibitory Effect on the *T. cruzi* Fe-SOD Enzyme. In previous work we had found that benzo[*g*]phthalazine derivatives containing sp^2 or sp^3 nitrogen atoms in the side chains and other pyrazole-containing related structures were able to inhibit the activity of the Fe-SOD enzyme of the parasite, and the inhibiting features had been related to the high complexing potentiality of the polyaminic structures assayed, since the environment of the active site could be modified by complexation.[20−23,25]

Therefore, the effects of compounds **1−4** on *T. cruzi* Fe-SOD were assayed at concentrations ranging from 1 to 100 μM. Epimastigote forms of *T. cruzi* which excreted Fe-SOD when cultured in a medium lacking inactive fetal calf serum (FCS)

dx.doi.org/10.1021/jm3011004 | J. Med. Chem. 2012, 55, 9900−9913

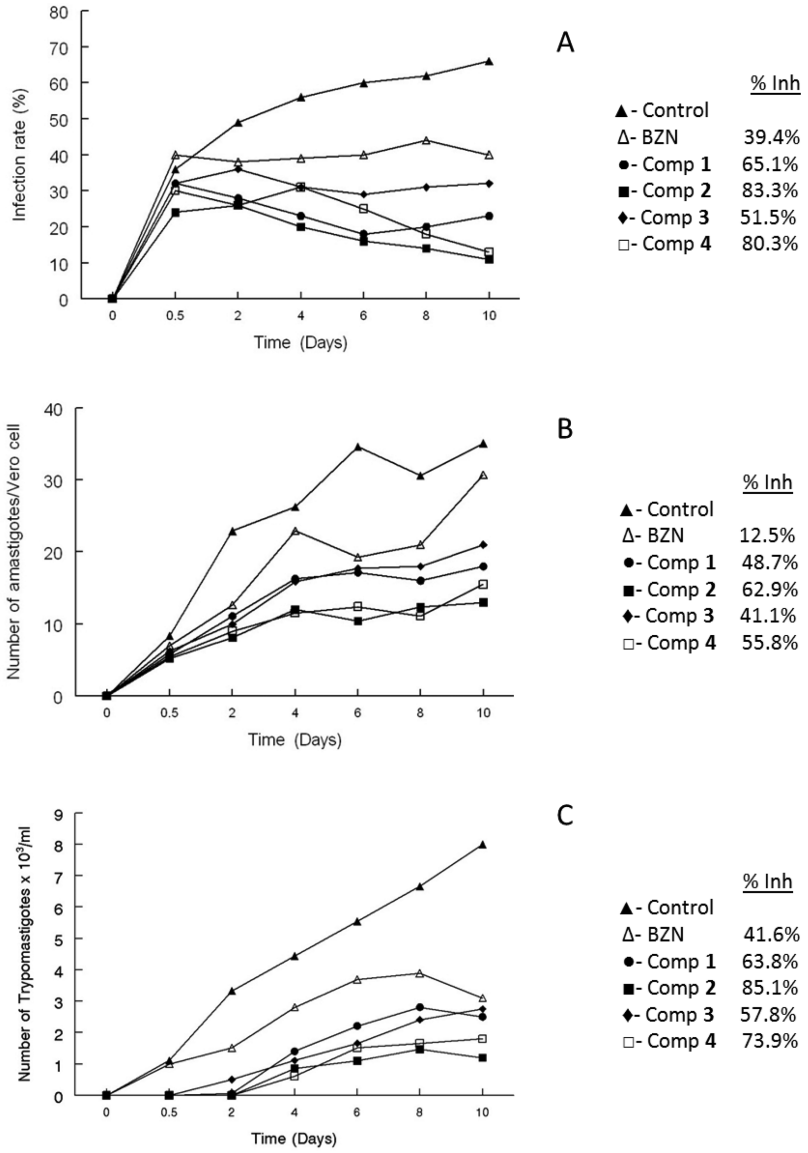

Figure 3. Effect of the imidazole-containing phthalazine derivatives **1**–**4** on the infection rate and growth of *T. cruzi*: (A) rate of infection; (B) mean number of amastigotes per infected Vero cell; (C) number of trypomastigotes in the culture medium for (▲) control, (△) BZN, (●) **1**, (■) **2**, (◆) **3**, (□) **4**. Measured at IC_{25}. Values are the means of three separate experiments.

were used.[26] The inhibition data obtained are shown in Figure 4A, and the corresponding IC_{50} values are included in order to make the interpretation of results easier. For comparison, Figure 4B shows the effect of the same compounds on CuZn-SOD obtained from human erythrocytes. A simple visual comparison of Figure 4A and Figure 4B revealed that Fe-SOD was clearly inhibited, whereas the inhibition of human CuZn-SOD was substantially lower. Results were especially noteworthy for the monosubstituted compounds **2** and **4** (which also showed the best in vitro activity results), since both of them reached 100% inhibition of Fe-SOD even at 50 μM. Concerning the IC_{50} data, the four compounds showed lower values for Fe-SOD than for CuZn-SOD, and **2** and **4** were 5.5-fold and 5.8-fold more inhibitory against Fe-SOD than against human SOD, respectively, whereas much lower differences were found for **1** and **3** (2.6-fold and 1.6-fold, respectively). On the other hand, when the monosubstituted derivatives were assayed against Fe-SOD, lower IC_{50} values were obtained than in the case of their disubstituted counterparts (12.89 μM against 48.03 μM for the couple **2** and **1**, and 14.36 μM against 41.66 μM for **4** and **3**).

In order to obtain more information on the activity shown by the tested compounds over Fe-SOD, a tentative molecular modeling study on their mode of interaction with the enzyme was performed. It is known that Fe-SOD enzymes are formed by two monomers, both of which contain a non-heme iron as a five-coordinated active site ligated by three histidine units, an aspartate group, and an axial H_2O or HO^- ligand supported by an essential conserved H-bonding network comprising amino acids and extending across the interface to the other monomer of the Fe-SOD dimer.[27] Specifically, the coordinated solvent engages in a H-bond with the Asp160 ligand and another engages with the conserved active site Gln69[28] (Figure 5A). Several studies have emphasized the importance of that ligand and its hydrogen-bonding partners in tuning the antioxidant activity of Fe-SOD.[29] It acts as a proton donor/acceptor, thereby facilitating the release of peroxide generated in the reduction of the substrate,[28] and it also plays a critical role in

dx.doi.org/10.1021/jm3011004 | J. Med. Chem. 2012, 55, 9900–9913

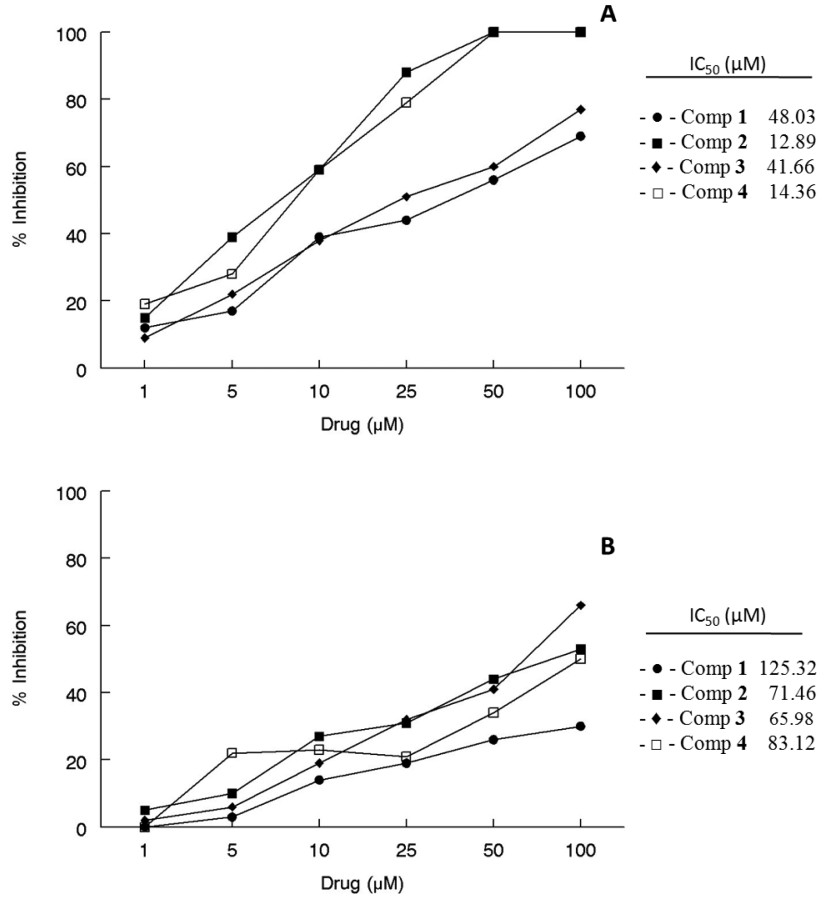

Figure 4. (A) In vitro inhibition (%) of Fe-SOD in *T. cruzi* epimastigotes for compounds **1**−**4** (activity, 20.77 ± 3.18 U/mg). (B) In vitro inhibition of CuZn-SOD in human erythrocytes for compounds **1**−**4** (activity, 23.36 ± 14.21 U/mg). Values are the average of five separate determinations. Differences between the activities of the control homogenate and those incubated with compounds **1**−**4** were obtained according to the Newman−Keuls test. IC_{50} was calculated by linear regression analysis from the K_c values at concentrations used (1, 10, 25, 50, and 100 μM).

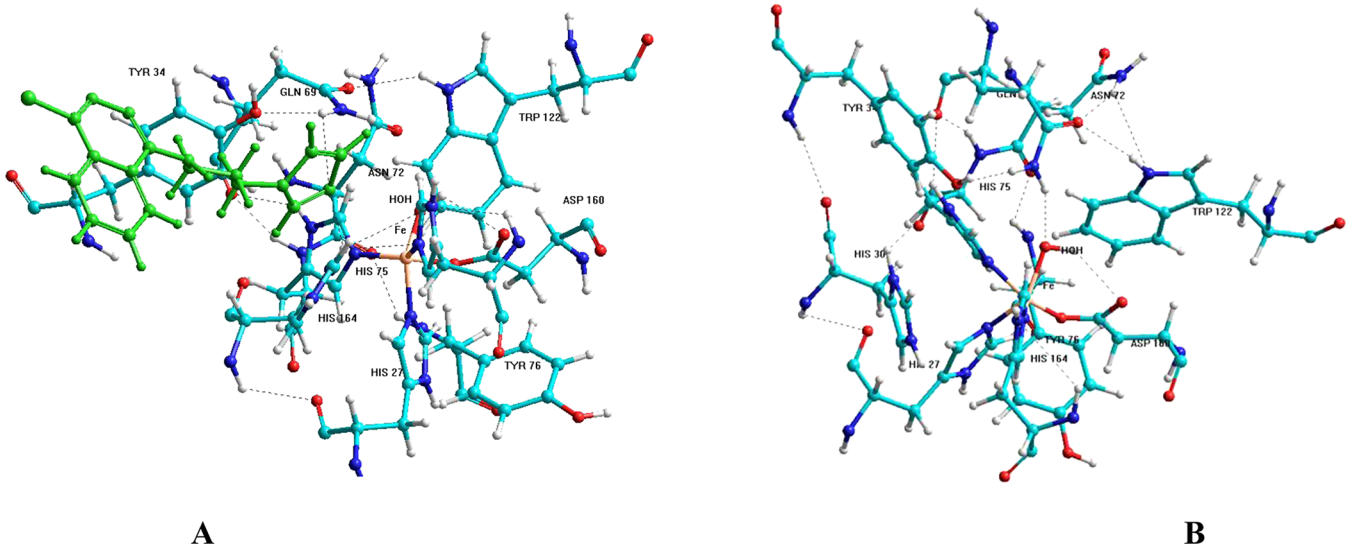

Figure 5. Molecular models of the free Fe-SOD enzyme active site with the supporting network of hydrogen bonds (A) and the same active site with compound **4** embedded in the proximity of the iron atom with the hydrogen-bonding network modified (B).

modulating the reduction potential of the iron center.[29] It is believed that a turnover mechanism takes place between the Fe^{3+}/HO^- and Fe^{2+}/H_2O pairs, since uptake of an electron is coupled to the acquisition of a proton, and the proton released upon reoxidation of iron contributes to the product formation.[30] In that scheme, the protonation state of the coordinated solvent is supposed to be strongly influenced by H-bonding with Gln69, which in turn H-bonds to a network including Tyr34, Asn72, and Trp122, among others. On that basis, it has been proposed that enzyme inhibition could take

dx.doi.org/10.1021/jm3011004 | J. Med. Chem. 2012, 55, 9900−9913

place by modification of the H-bonding system induced by the presence of a different ligand.[31]

The ability of related benzo[*g*]phthalazine derivatives to interact with a single strand of Fe-SOD had been previously tested by us using the AMBER force field implemented in Hyperchem 8.0,[22] so the methodology was applied to the complete structure of the Fe-SOD enzyme obtained from the Brookhaven Proteine Data Bank 2gpc entry. Figure 5A shows the active site moiety of the Fe-SOD enzyme obtained as specified in the Experimental Section, with the hydrogen-bonding system outlined above displayed as dashed lines and the solvent ligand in the foreground linked to the iron atom. The interactions with Gln69 and Asp160 are clearly seen. When intoducing the monoalkylamino substituted compound **4** (with a side chain that is longer than that of **2**), approaching the active site took place through the interface between the two monomers of the enzyme, and the side chain was buried into one monomer and located between the tyrosine residue and the iron atom, with the imidazole sp^2 nitrogen N-3′ pointing toward the metal ion in the most favored disposition (Figure 5B). As a consequence, the hydroxyl ligand was displaced a little apart from its initial position, and the H-bonding pattern seemed to be completely distorted, with Gln69 located too far from the HO^- group to form a stable hydrogen bond and interacting instead with the imidazole nitrogen. We think that these findings could explain in part the enzyme deactivation found experimentally.

In order to complement the molecular modeling results commented above, the most favored distance between the iron atom and the imidazole nitrogen atom N-3′ for compounds **1**−**4** was also calculated. It was shown that the N-3′ nitrogen of the dialkylamino substituted compounds **1** and **3** was located further away than that of the respective monoalkylamino substituted analogues **2** and **4**: 0.409 and 0.368 nm for **1** and **3** against 0.394 and 0.343 nm for **2** and **4**, suggesting that the less bulky (and more active) compounds **2** and **4** are inserted deeper into the active site. On the other hand, compound **4**, with the longest side chain, is located closer to the iron atom than **2**, so the chain length could be a factor favoring approach to the active site core. According to this, the synthesis of a series of phthalazine derivatives with variable chain lengths is planned in order to more accurately evaluate the effect of that modification on anti-*T. cruzi* activity.

In Vivo Anti-*T. cruzi* Activity in the Acute Phase of Chagas Disease. Since the monosubstituted compounds **2** and **4** showed remarkable SI values with respect to BZN in the in vitro experiments and were also the best inhibitors of the parasitic Fe-SOD enzyme, they were selected for performing further in vivo estudies in the chosen murine model. Their trypanocidal activity during the acute phase of Chagas disease [until 40 days postinfection (pi)] was first investigated. Different groups of female Balb/c mice were inoculated with 5×10^5 metacyclic blood trypomastigotes of SN3 *T. cruzi*, and the infection started. We opted for the intraperitoneal doping route, which usually leads to lower mortality rates than the intravenous procedure,[32] and testing compounds doses of 5 and 15 mg/kg body weight were administered every day from the seventh day of infestation until day 12 pi. The 5 mg/kg dose was selected in order to allow comparison of the parasitemia data with those obtained previously for related structures.[22] The 15 mg/kg dose had the purpose of pondering the effect of an increment of the dose on the parasitemia levels and the mortality of mice. Parasite counting was performed on 5 μL blood samples obtained from the mandibular vein. None of the animals treated with either the control or compounds **2** and **4** died during the treatment. However, similar assays performed in the presence of BZN always led to mice mortality values of about 20%. As shown in Figure 5, the reduction of parasitemia in mice treated with compounds **2** and **4** was evident as early as the very beginning of treatment and was maintained until days 15−20 pi. A decrease in the trypomastigote numbers per infected cell was more intense in assays performed with the highest dose of the testing compounds (15 mg/kg body weight). However, on day 15 pi the four assays provided very similar trypomastigote numbers, resulting in parasitemia reduction values between 59% and 64% with respect to the control experiment. Although benznidazole graphic data have not been included in Figure 6 for easier visualization, it must be noted that parasitemia reductions originated by BZN at the 5 mg/kg body weight dose were much smaller (15.3% on day 15 pi and 16.7% on day 40 pi). After day 25 pi, the parasitemia levels began to decrease again rapidly in all cases, and when the highest dose was used, low numbers of the parasitic trypomastigotes were found at day 40 pi for the two compounds. On the whole, the behavior of **2** and **4** was similar and both of these compounds were effective in the acute phase at the concentrations selected. However, compound **2** was, in general, more efficient in the reduction of parasitemia than compound **4**, especially when the 15 mg/kg concentration was tested (with a parasitemia reduction value on day 40 pi as high as 74%, in contrast with the 61% reduction found for compound **4** on the same day).

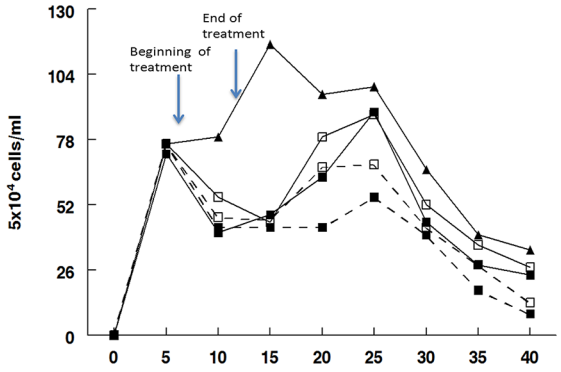

Figure 6. Parasitemia in the murine model of acute Chagas disease: control (▲) and dose receiving 5 mg/kg (continuous lines) and 15 mg/kg (dashed lines) of compound **2** (■) and compound **4** (□).

The next step was to evaluate the behavior of compounds **2** and **4** in the chronic phase, in which the positive effect of the current drugs is under much discussion.[9] Above it is stated that the high reactivation ability of the parasitemia in immunocompromised individuals cured of Chagas disease with apparent success was a major problem. Therefore, the mice treated as described above were taken up to day 120 pi (advanced chronic phase) and were subsequently divided into two subgroups: one of them was maintained under the same conditions without further treatment, while the other was subjected to three successive cycles of immunosuppression with cyclophosphamide monohydrate for 3 consecutive weeks, as described in the Experimental Section.[33] In order to evaluate the immune status and the disease extent of the mice at that stage, blood samples were extracted for determining the parasitemia and immunoglobulin G (IgG) levels in comparison with the corresponding

nonimmunosuppressed (control) subgroup of mice. Concerning the parasitemia assay, the number of parasites was counted from blood extracted on the day after finishing the three immunosuppresion cycles, and the same procedure used in the acute phase was followed. The enzyme-linked immunosorbent assay (ELISA) was used for the detection of IgG levels,[34] and the antigen source was the Fe-SOD enzyme isolated in our laboratory. The detection of total IgG allows the evaluation of the immune status of the mice, since that protein indicates the level of protection that should be attributed to the tested compounds, as well as the innate protection that mice have naturally. It has been described that the IgG levels are stable in the chronic phase and close to the baseline.[35] Table 3 (column A) shows that the stability of IgG levels was achieved in the nonimmunosuppressed mice, with the control optical density (OD) values falling inside the calculated standard deviation (SD) of the group. However, the control OD, measured for the immunosuppressed mice, was much higher than the corresponding mean plus the calculated SD, confirming a greater presence of the parasite. If the Δ_{B-A} values obtained for compounds **2** and **4** are compared, it is clear that they led to a decrease in the infection revival. As expected, the best results were obtained with the higher 15 mg/kg dose, and it was also shown that compound **2** was more effective than **4** for the two concentrations tested, in accordance with the results obtained in the acute phase.

Table 3. OD Values Obtained in the ELISA Experiment for Compounds 2 and 4 on Day 150 pi for the Different Groups of Mice Assayed[a]

	A	B	Δ_{B-A}
control	0.1089	0.1306	0.0217
2 (5 mg/kg)	0.1019	0.1130	0.0103
4 (5 mg/kg)	0.1027	0.1162	0.0143
2 (15 mg/kg)	0.1080	0.1150	0.0067
4 (15 mg/kg)	0.1083	0.1176	0.0096
mean ± SD	0.1060 ± 0.0030	0.1185 ± 0.0062	

[a]**A** = Group of non-immunocompromised mice; **B** = Group of immunocompromised mice; Δ_{B-A}=Differences between the OD values of the two groups. Values were obtained as an average of three independent experiments.

Results obtained from the ELISA experiments were confirmed by the parasitemia assay performed as indicated above. Figure 7 shows a very illustrative tridimensional graph indicating the percentage of parasitemia reactivation for compounds **2** and **4** at 5 and 15 mg/kg weight, in comparison with the control mice. Very low percentages were obtained in the four cases, with values ranging from 4% to 21%, whereas a reactivation of 63% was found in the control mice. BZN data obtained from the 80% mice that survived after treatment gave a substantially higher parasitemia reactivation of 36% at a weight of 5 mg/kg, indicating that the two tested compounds were clearly more efficient than the reference drug. In concordance with the ELISA test, compound **2** was more effective than **4** at both the lowest and highest doses assayed (9% and 4% reactivation for **2** against 21% and 8% for **4**, respectively).

Metabolite Excretion Study. Trypanosomatids are unable to completely degrade glucose to CO_2, so they excrete part of the hexose skeleton into the medium as partially oxidized fragments, whose nature and percentage depend on the pathway used for glucose metabolism.[36] The catabolism products in *T. cruzi* are mainly succinate, acetate, L-lactate, L-alanine, and ethanol.[37] In order to obtain some information about the effects of compounds **1**−**4** on the glucose metabolism of the parasite, the ^{1}H NMR spectra of *T. cruzi* epimastigotes treated with the testing compounds (spectra are included in the Supporting Information data sheet for consideration by the reader) were registered, the final excretion products were identified qualitatively and quantitatively, and the results obtained were compared with those found for untreated control epimastigotes. Table 4 shows the differences found in every case with respect to the control. Excretion of succinate was not affected in the presence of any of the four compounds with respect to the nontreated epimastigotes. However, the formation of acetate and L-lactate was substantially reduced in all cases, and the amounts of L-alanine and ethanol decreased in the most active monosubstituted compounds **2** and **4** but remained unaltered in their disubstituted analogues **1** and **3**. Even more, excretion of acetate and L-lactate decreased by a greater extent in **2** and **4** than in their respective disubstituted counterparts. On the basis of these data, it seems that the succinate pathway is not modified by the compounds assayed, but the acetate pathway is apparently affected, especially in the case of the most active compounds, which should interfere more effectively with the enzymes involved in the production of the corresponding metabolites. As described in recent studies, succinate is produced in both the glycosome and the mitochondrion from phosphoenolpyruvate (PEP) via malate and fumarate,[38] and the tested compounds do not seem to interact with either of those pathways. On the other hand, acetate, L-lactate, L-alanine, and ethanol originate from the

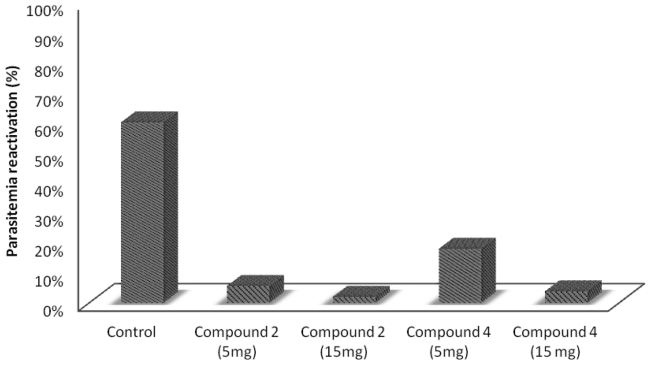

Figure 7. Reactivation percentage in mice after immunosuppression. Each group was compared with the nonimmunesuppressed group treated with the same compound and dosage. Values were obtained as an average of three independent experiments.

Table 4. Variation in the Height of the Peaks Corresponding to Catabolites Excreted by *T. cruzi* Epimastigotes in the Presence of Compounds 1−4 with Respect to the Control Test[a]

compd	Eth	Lac	Ala	A	S
1	=	−15%	=	−10%	=
2	−12%	−33%	−13%	−21%	=
3	=	−24%	=	−21%	=
4	−16%	−38%	−27%	−54%	=

[a]Eth, ethanol; Lac, L-lactate; Ala, L-alanine; A, acetate; S, succinate; (−) peak decreasing; (=) no difference detected.

dx.doi.org/10.1021/jm3011004 | J. Med. Chem. 2012, 55, 9900−9913

transformation of PEP in pyruvate in the presence of pyruvate kinase or pyruvate phosphate dikinase.[39] With the only exception of the more elaborate acetate pathway, the other three catabolites are formed directly from pyruvate in the cytosol. On the basis of data shown in Table 4, it would be possible that compounds **2** and **4** were interacting with the pyruvate kinase enzymes and modifying the glucose metabolism of the parasite at the pyruvate stage.

Ultrastructural Alterations. The remarkable trypanosomicidal activity shown by compounds **1**−**4** should cause important damage in the parasite cells. Therefore, the morphological alterations caused in *T. cruzi* Maracay epimastigotes were analyzed using TEM, in order to obtain some information about the way in which the cell structure was affected. The most significant variations compared to the control cells are shown in Figure 8 for parasites treated with **1**−**4**. As expected, highly significant alterations were shown by all four compounds tested. A large number of parasites died, and deep modifications were evident in most of the rest. As a general rule, many cytoplasms were completely filled with vacuoles, and many other were electron dense. The shape of many parasites was heavily distorted, with some reduced in size and others very swollen (second to fifth panels in Figure 8). In particular, parasites treated with compound **2** also showed large flagellar pockets (third panel in Figure 8), and those assayed with **3** were characterized by nuclear membranes that were fully altered and separated into two units with a significant space between them (fourth panel in Figure 8). In the case of compound **4**, mitochondria were frequently swollen, and epimastigotes with granular and membranous cytoplasms and bulky vacuoles were common. The cytoplasms were extremely disorganized (fifth panel in Figure 8). The disubstituted derivative **1** appeared to affect the cells to a lesser extent than the other compounds, but even in that case nearly 50% of the parasites still died, and many empty zones were observed in the cytoplasms (second panel in Figure 8). All of these observations regarding essential damage in the parasite cells agree with the significant activity found for compounds **1**−**4**.

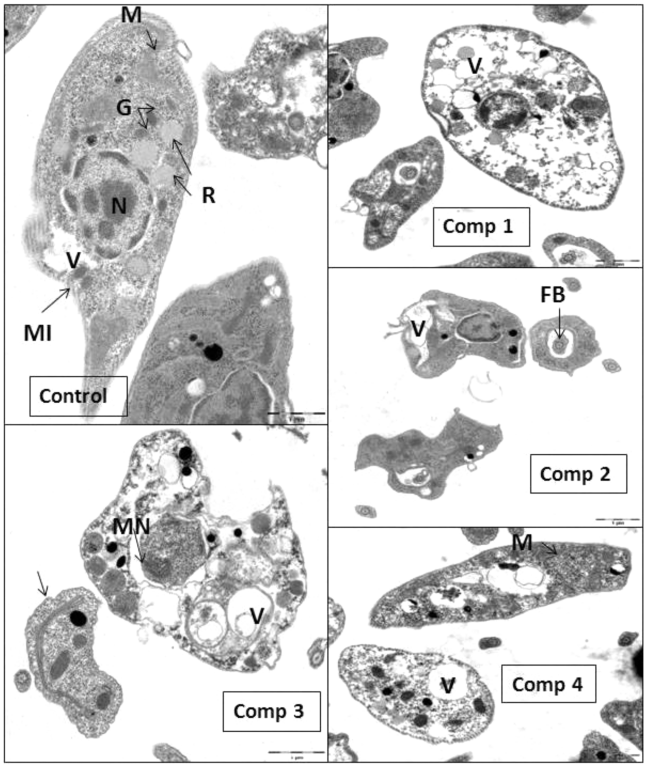

Figure 8. Ultrastructural alterations by TEM in epimastigotes of *T. cruzi* Maracay that were either untreated (control) or treated with compounds **1**−**4**, showing organelles with their characteristics: parasite nucleus (N), reservosomes (R), vacuoles (V), mitochondrion (M), glycosomes (G), cytoskeleton microtubules (MI), large flagellar pockets (FB), parasite size reduction (arrow), altered nuclear membrane (MN): (control) untreated parasites, bar 1 μm; (Comp 1) parasites treated with compound **1**, bar 1 μm; (Comp 2) parasites treated with compound **2**, bar 1 μm; (Comp 3) parasites treated with compound **3**, bar 1 μm; (Comp 4) parasites treated with compound **4**, bar 1 μm.

From the results of this work, it can be concluded that the imidazole-based monoalkylaminophthalazine derivatives **2** and **4** showed remarkable in vitro and in vivo trypanosomicidal activity, being especially active against the acute phase of Chagas disease. These compounds also showed a much lower level of toxicity in Vero cells than BZN, and they were almost inactive against human SOD but active against the Fe-SOD of the parasite. Furthermore, both of these compounds substantially decreased the parasitemia reactivation in immunocompromised mice, and reactivation at the higher dose was negligible in the case of **4**, which is an unusual characteristic in most of the commonly prescribed drugs against Chagas disease. These tentative results suggest the convenience of performing further histopathological studies on target organs, which will be the object of a next publication. On this basis, we believe that both compounds fulfill the requirements for performing a more detailed study of the nature of the mechanisms involved in their activity patterns and, furthermore, that they are serious candidates for studying antiparasitical activity at a higher level.

EXPERIMENTAL SECTION

Chemistry. The starting amines 3-(imidazol-1-yl)propylamine and 2-(imidazol-4-yl)ethylamine (histamine) were purchased from Sigma-Aldrich and used without further purification. 1,4-Dichlorophthalazine was obtained from commercial phthalhydrazide (Sigma-Aldrich) following a standard method.[40] Solvents were dried using standard techniques.[41] All of the reactions were monitored using thin layer chromatography (TLC) on precoated aluminum sheets of silica gel $60PF_{254}$ (Merck, layer thickness 0.2 mm). Compounds were detected with UV light (254 nm). Chromatographic separations were performed on columns in the indicated solvent system using flash chromatography on silica gel (particle size 0.040−0.063 mm). Melting points were determined in a Gallenkampf apparatus and were uncorrected. ^{1}H NMR spectra were recorded on a Bruker 300 and a Variant XL 300 at 300 MHz, and ^{13}C NMR spectra were recorded at 75 MHz at room temperature employing DMSO-d_6 as the solvent. Chemical shifts were reported in ppm (δ scale) from tetramethylsilane (TMS). All assignments were performed on the basis of ^{1}H−^{13}C heteronuclear multiple quantum coherence experiments (gHMQC). IR spectra were recorded on a Perkin-Elmer 257 spectrometer (4000−400 cm^{-1} range). Electrospray mass spectra were recorded with a Hewlett-Packard 1100 MSD apparatus. Elemental analyses were performed in a Perkin-Elmer 2400-CHN instrument by the CAI of Microanalisis, Universidad Complutense, Madrid, Spain. Elemental analysis was used to ascertain a purity higher than 95% for all the biologically tested compounds.

Synthesis of 1 and 3 (Method A). A solution of 1,4-dichlorophthalazine, the corresponding aminoalkylimidazole, and triethylamine in xylene was heated at 120 °C for several hours. The reaction mixture was cooled to room temperature and the solvent removed under reduced pressure. The solid residue was purified by

column chromatography with a polarity-increasing chloroform/methanol/ammonium hydroxide mixture as the eluent to obtain the desired product.

1,4-Bis[2-(imidazol-4-yl)ethylamino]phthalazine (1). This compound was prepared by heating 1,4-dichlorophthalazine (450 mg, 2.26 mmol), 2-(imidazol-4-yl)ethylamine (500 mg, 4.50 mmol), and triethylamine (1.36 g, 13.5 mmol) in 45 mL of xylene during 6 h. Further workup and purification of the reaction mixture afforded 200 mg (21%) of a solid which was identified as **1**·2HCl (R_f = 0.52, $CHCl_3$/MeOH/NH_4OH, v/v 8/2/1), mp 198−200 °C. IR (KBr) = 3722, 3169, 1928, 1742, 1636, 1545, 1482, 1359, 1223, 945, 775 cm^{-1}. ^1H NMR (DMSO-d_6): δ 8.44 (m, 2H, H-5, H-8), 8.03 (m, 2H, H-6, H-7), 7.81 (s, 2H, H-2′), 6.99(s, 2H, H-5′), 3.66 (t, 4H, Hα), 2.97 (t, 4H, Hβ) ppm. ^{13}C NMR (DMSO-d_6): δ 148.02 (C-1, C-4), 134.54/134.42 (C-2′, C-4′), 134.02 (C-6, C-7), 124.04 (C-5, C-8), 121.25 (C-4a, C8a), 116.31 (C-5′), 42.33 (Cα), 25.14 (Cβ) ppm. MS-ESI (MeOH): m/z (%): 349 (MH^+ − 2HCl, 100). Anal. ($C_{18}H_{20}N_8$·2HCl·5H_2O) C, H, N.

1,4-Bis[3-(imidazol-1-yl)propylamino]phthalazine (3). This compound was prepared by heating 1,4-dichlorophthalazine (1.45 g, 7.28 mmol), 3-(imidazol-1-yl)propylamine (1.90 g, 14.52 mmol), and triethylamine (1.37 g, 13.8 mol) in 60 mL of xylene during 24 h. Further workup and purification of the reaction mixture afforded 525 mg (16%) of a solid which was identified as **3**·2HCl (R_f = 0.11, $CHCl_3$/MeOH/NH_4OH, v/v 8/2/1), mp 190−192 °C. IR (KBr) = 3669, 3405, 3213, 3107, 2960, 1641, 1562, 1515, 1371,1342, 1235, 1091, 662 cm^{-1}. ^1H NMR (DMSO-d_6): δ 8.89 (m, 2H, H-5, H-8), 8.17 (m, 2H, H-6, H-7), 7.75 (s, 2H, H-2′), 7.22 (s, 2H, H-5′), 6.96 (s, 2H, H-4′), 4.25 (t, 4H, Hγ), 3.53 (t, 4H, Hα), 2.31 (m, 4H, Hβ) ppm. ^{13}C NMR (DMSO-d_6): δ 148.43 (C-1, C-4), 137.50 (C-2′), 132.67 (C-6, C-7), 128.15 (C-4′), 124.03 (C-5, C-8), 121.12 (C-5′), 119.80 (C-4a, C-8a), 43.99 (Cγ), 38.77 (Cα), 29.52 (Cβ) ppm. MS-ESI (MeOH), m/z (%): 377 (MH^+ − 2HCl, 100). Anal. ($C_{20}H_{24}N_8$·2HCl·H_2O) C, H, N.

Synthesis of 2 and 4 (Method B). A solution of 1,4-dichlorophthalazine, the corresponding aminoalkylimidazole, and sodium carbonate in acetonitrile was heated to reflux for several hours. The reaction mixture was cooled to room temperature, and a solid containing the reaction products and potassium carbonate was separated by filtration and extracted three times with chloroform. The organic solution was evaporated under reduced pressure and the residue was purified by flash column chromatography with a polarity increasing chloroform/methanol mixture as eluent to obtain the desired product.

1-[2-(Imidazol-4-yl)ethylamino]-4-chlorophthalazine (2). This compound was prepared by heating 1,4-dichlorophthalazine (895 mg, 4.50 mmol), 2-(imidazol-4-yl)ethylamine (500 mg, 4.50 mmol), and potassium carbonate (3.10 g, 29.2 mmol) in 70 mL of acetonitrile during 72 h. Further workup and purification of the reaction mixture afforded 200 mg (16%) of a solid which was identified as free **2** (R_f = 0.45, $CHCl_3$/MeOH, v/v 8/2), mp 158−160 °C. IR (KBr) = 3219, 3102, 2886, 2932, 1731, 1576, 1525, 1484, 1362, 1181, 981, 769 cm^{-1}. ^1H NMR (DMSO-d_6): δ, 8.33 (m, 1H, H-8), 8.05 (m, 1H, H-5), 8.02 (m, 2H, H-6, H-7), 7.59 (s, 1H, H-2′), 6.88 (s, 1H, H-5′), 3.79 (t, 2H, Hα), 2.95 (m, 2H, Hβ) ppm. ^{13}C NMR (DMSO-d_6): δ: 154.01 (C-1), 143.96 (C-4), 134.59 (C-2′/C-4′), 132.59/132.50 (C-6/C-7), 125.26 (C-4a), 124.48 (C-8), 122.76 (C-5), 120.00 (C-8a), 116.70 (C-5′), 41.35 (Cα), 25.97 (Cβ) ppm. MS-ESI (MeOH): m/z (%): 273 (M^+, 100). Anal. ($C_{13}H_{12}N_5Cl$·H_2O) C, H, N.

1-[3-(Imidazol-1-yl)propylamino]-4-chlorophthalazine (4). This compound was prepared by heating 1,4-dichlorophthalazine (200 mg, 0.995 mmol), 3-(imidazol-1-yl)propylamine (124 mg, 0.995 mmol), and potassium carbonate (1.37 g, 12.9 mmol) in 70 mL of acetonitrile during 45 h. Further workup and purification of the reaction mixture afforded 138 mg (48%) of a solid which was identified as free **4** (R_f = 0.52, $CHCl_3$/MeOH, v/v 8/2), mp 183−185 °C. IR (KBr) = 3666, 3216, 3107, 2964, 2932, 1679, 1574, 1520, 1416, 1286, 1178, 1106, 799, 660 cm^{-1}. ^1H NMR (DMSO-d_6): δ, 8.68 (m, 1H, H-8), 8.50 (m, 1H, H-5), 8.17 (m, 2H, H-6, H-7), 7.65 (s, 1H, H-2′), 7.21 (s, 1H, H-5′), 6.95 (s, 1H, H-4′), 4.22 (t, 2H, Hγ), 3.64 (t, 2H, Hα) 2.30 (m, 2H, Hβ) ppm. ^{13}C NMR (DMSO-d_6): δ 154.13 (C-1), 144.14 (C-4), 137.60 (C-2′), 132.90/132.49 (C-6/C-7), 128.4 (C-4′), 125.25 (C-4a), 124.49 (C-8), 122.88 (C-5), 120.00 (C-8a), 119.50 (C-5′), 44.01(Cγ), 38.46(Cα), 29.84(Cβ) ppm. MS-ESI (MeOH), m/z (%): 287 (M^+, 100). Anal. ($C_{14}H_{14}N_5Cl$) C, H, N.

Parasite Strain, Culture. *Trypanosoma cruzi* SN3 strain of IRHOD/CO/2008/SN3 was isolated from domestic *Rhodnius prolixus*; biological origin is Guajira (Colombia).[42] Epimastigote forms were grown in axenic Grace's insect medium (Gibco) supplemented with 10% inactivated fetal bovine serum (FBS) at 28 °C in tissue-culture flasks. In order to obtain the parasite suspension for the trypanocidal assay, the epimastigote culture (in the exponential growth phase) was concentrated by centrifugation at 400*g* for 10 min and the number of flagellates was counted in a hemocytometric chamber.

Transformation of Epimastigotes to the Metacyclic Form. Metacyclogenesis was induced by culturing the parasites at 28 °C in modified Grace's medium (Gibco) for 12 days, as described previously.[43] Twelve days after cultivation at 28 °C, metacyclic forms were counted in a Neubauer hemocytometric chamber. The proportion of metacyclic forms was around 40% at this stage.

Cell Culture and Cytotoxicity Tests. Vero cells (Flow) were grown in Roswell Park Memorial Institute (RPMI) medium (Gibco), supplemented with 10% inactivated FBS, in a humidified 95% air, 5% CO_2 atmosphere at 37 °C for 2 days. For the cytotoxicity testing, cells were placed in 25 mL Colie-based bottles (Sterling) and centrifuged at 100*g* for 5 min. The culture medium was removed, and fresh medium was added to a final concentration of 1 × 10^5 cells/mL. This cell suspension was distributed in a culture tray (with 24 wells) at a rate of 100 μL/well and incubated for 2 days at 37 °C in a humidified atmosphere enriched with 5% CO_2. The medium was removed, and fresh medium was added together with each test compound (at concentrations of 100, 50, 25, 10, and 1 μM). After 72 h of treatment, cell viability was determined by flow cytometry according to a methodology described by us.[44]

In Vitro Activity Assays: Extracellular Forms. *Epimastigote Assay.* Epimastigotes were collected in the exponential growth phase and distributed in culture trays (with 24 wells) at a final concentration of 5 × 10^4 parasites/well. The compounds to be tested and benznidazole were dissolved in medium trypanosomes liquid (MTL) and were tested at 100, 50, 25, 10, and 1 μM. The effects of the different concentrations of each compound against the epimastigotes were tested for 72 h using a Neubauer hemocytometric chamber. The trypanocidal effect is expressed as IC_{50}, i.e., the concentration required to result in 50% inhibition, as calculated by linear-regression analysis from the K_c of the concentrations used.

In Vitro Activity Assays: Intracellular forms. *Axenic Amastigotes Assay.* Axenic amastigotes of *T. cruzi,* were cultured following the methodology described previously by Moreno et al.[45] Thus, the epimastigote transformation to amastigotes was achieved after 3 days of culture in M199 medium (Invitrogen, Leiden, The Netherlands) supplemented with 10% heat-inactivated FCS, 1 g/L β-alanine, 100 mg/L L-asparagine, 200 mg/L saccharose, 50 mg/L sodium pyruvate, 320 mg/L malic acid, 40 mg/L fumaric acid, 70 mg/L succinic acid, 200 mg/L α-ketoglutaric acid, 300 mg/L citric acid, 1.1 g/L sodium bicarbonate, 5 g/L 4-morpholinoethanesulfonic acid (MES), 0.4 mg/L hemin, and 10 mg/L gentamicine, pH 5.4, at 37 °C. The effect of each compound against the axenic amastigotes was tested for 48 h using a Neubauer hemocytometric chamber. The trypanocidal effect is expressed as IC_{50}, i.e. the concentration required to result in 50% inhibition, as calculated by linear-regression analysis from the K_c of the concentrations used.

Amastigotes Assay. Vero cells were cultured in RPMI medium in a humidified 95% air and 5% CO_2 atmosphere at 37 °C. The cells were seeded at a density of 1 × 10^4 cells/well in 24-well microplates (Nunc) with rounded coverslips on the bottom and then cultivated for 2 days. Afterward, adhered Vero cells were infected in vitro with metacyclic forms of *T. cruzi* at a ratio of 10:1 and maintained for 24 h at 37 °C in 5% CO_2 in air. The extracellular parasites were removed by washing,

dx.doi.org/10.1021/jm3011004 | J. Med. Chem. 2012, 55, 9900−9913

and the infected cultures were incubated with the compounds (1, 10, 25, 50, and 100 μM) and cultured for 72 h in RPMI and 10% inactivated fetal bovine serum. The activity of the compounds was determined from the percentage reduction in the number of amastigotes in the treated and untreated cultures in methanol-fixed and Giemsa-stained preparations. The values are the mean of four separate determinations.[46] The trypanocidal effect was expressed as IC_{50}.

Blood Trypomastigotes Assay. Compounds **1**−**4** were also evaluated on blood trypomastigote forms of *T. cruzi*. BALB/c mice infected with *T. cruzi* were used 7 days after infection. Blood was obtained by cardiac puncture using 3.8% sodium citrate as anticoagulant in a 7:3 blood/anticoagulant ratio. The parasitemia in the infected mice was about 1×10^5 parasites/mL. The compounds were diluted in phosphate-buffered saline solution (PBS) to give a final concentration 10, 25, and 50 μM for each product. Aliquots (20 μL) of each solution were mixed in cultures trays (96 wells) with 55 μL of infected blood containing the parasites at a concentration near 1×10^6 parasites/mL. Infected blood with PBS, at the same concentrations as the products, was used as control. The plates were shaken for 10 min at room temperature and kept at 4 °C for 24 h. Each solution was examined microscopically (Olympus CX41) for parasite counting using the Neubauer hemocytometric chamber (a dilution of 1:100 in PBS was necessary to get into the range of counting). The activity (percent of parasites reduction) was compared with that of the control.

Infectivity Assay. Vero cells were cultured in RPMI medium as described above. Afterward, the cells were infected in vitro with metacyclic forms of *T. cruzi* at a ratio of 10:1. The test compounds (IC_{25} concentrations) were added immediately after infection and incubated for 12 h at 37 °C in a 5% CO_2 atmosphere. The extracellular parasites and the test compounds were removed by washing, and the infected cultures were grown for 10 days in fresh medium. Fresh culture medium was added every 48 h. The activity of each compound tested was determined from the percentage of infected cells and the number of amastigotes per infected cell in treated and untreated cultures in the methanol-fixed and Giemsa-stained preparations. The percentage of infected cells and the mean number of amastigotes per infected cell were determined by analyzing more than 100 host cells distributed throughout randomly chosen microscopic fields. The values are the mean of four separate determinations. The number of trypomastigotes in the medium was determined as previously described.[43]

SOD Enzymatic Inhibition. The parasites cultured as described above were centrifuged. The pellet was suspended in 3 mL of sodium chloride-Tris-EDTA (STE) buffer [0.25 M sucrose, 25 mM Tris-HCl, 1 M ethylendiaminetetraacetic acid (EDTA), pH 7.8] and disrupted by three cycles of sonic disintegration, 30 s each at 60 V. The sonicated homogenate was centrifuged at 1500*g* for 5 min at 4 °C, and the pellet was washed three times in ice-cold STE buffer. This fraction was centrifuged (2500*g* for 10 min at 4 °C), and the supernatant was collected. The protein concentrations were determined using the Bradford method.[47] Iron and copper−zinc superoxide dismutase (Fe-SOD and CuZn-SOD) activities were determined using the method described by Beyer and Fridovich,[48] which measures the reduction in nitroblue tetrazolium (NBT) by superoxide ions. Into each bucket, an amount of 845 μL of stock solution [3 mL of L-metionine (300 mg, 10 mL^{-1}), 2 mL of NBT (1.41 mg, 10 mL^{-1}), and 1.5 mL of Triton X-100 1% (v/v)] was added, along with 30 μL of the parasite homogenate fraction, 10 μL of riboflavine (0.44 mg, 10 mL^{-1}), and an equivalent volume of the different concentrations of the compounds tested. Five different concentrations were used for each product: 1, 2.5, 5, 12.5, and 25 μM (equivalent to 5, 12.5, 25, 62, and 125 μL, respectively, of the Stock solution). In the control experiment the volume was made up to 1000 μL with 50 mM potassium phosphate buffer (pH 7.8, 3 mL), whereas 30 μL of the parasite homogenate fraction was added to the mixtures containing the compounds. Then the absorbance (A_0) was measured at 560 nm in a spectrophotometer. Following this, each bucket was illuminated with UV light for 10 min under constant stirring and the absorbance (A_1) was measured. The human CuZn-SOD, coenzymes, and substrates used in these assays were obtained from Sigma Chemical Co. The data obtained were analyzed using the Newman−Keuls test.

Molecular Modeling. Molecular modeling studies were carried out using the AMBER method implemented in the HyperChem Professional 8.0 package,[49] modified by the inclusion of appropriate parameters.[50] Starting structures for compounds **1**−**4** were built by using HyperChem capabilities. Its geometry was minimized to a maximum energy gradient of 0.1 kcal/mol with the AMBER force field, using the Polak−Ribiere (conjugate gradient) minimizer, and a "simulated annealing" procedure was used to cover all conformational space. The most stable extended geometry was always used in all calculations of interaction with the enzyme. To mimic the conditions used in the activity measurements, i.e., water as solvent, all calculations were carried out in vacuo with a distance dependent dielectric constant. Charge assignments for all atoms were done by means of ab initio calculations using STO-3G basis set, as it is compatible with AMBER force field, prior to energy minimization using AMBER. The *T. cruzi* Fe-SOD enzyme structure was obtained from the Brookhaven Protein Data Bank (2gpc) and its energy minimized in the same way. Interaction studies were performed starting from structures with the compound positioned in the border of the enzyme cavity. Entering the cavity was forced using a restraint to the N−Fe distance, slowly decreasing this distance, and letting the complex achieve the minimum energy conformation with no restraints, for all the small driving steps, using the same conditions mentioned above.

In Vivo Trypanosomicidal Activity Assay. This experiment was performed using the rules and principles of the international guide for biomedical research in experimental animals and with the approval of the ethical committee of the University of Granada, Spain. Groups of six BALB/c albino female mice (6−8 weeks old, 25−30 g weight), maintained under standard conditions, were inoculated via the intraperitoneal route (bloodstream) with 5×10^5 metacyclic *T. cruzi* trypomastigotes obtained from previously infected mice blood. The animals were divided as follows: I, positive control group (mice infected but not treated); II, study group (mice infected and treated with two different concentrations of the compounds under study, one sublot per every concentration tested). An assessment of the effect of the compounds on the level of parasitemia after treatment (in acute and chronic phases) was performed by counting, as was an ELISA experiment (also comparing acute and chronic phases). For the acute phase assays, the administration of the testing compounds was begun on the seventh day of infestation once the infection was confirmed, and doses of 5 and 15 mg/kg body weight/day were used for 5 consecutive days (7−12 days postinfection). Peripheral blood was obtained from the mandibular vein of each treated mouse (5 μL samples) and dissolved in 495 μL of a PBS solution at a dilution of 1:100. The circulating parasite numbers were quantified with a Neubauer's chamber for counting blood cells. This counting was performed every 3 days during 40 days (acute phase). The number of metacyclic forms was expressed as parasites/mL. After day 60, the animals entered the chronic phase of the experiment, and on day 120 the mice were submitted to successive cycles of immunosuppression with cyclophosphamide monohydrate. The immunosuppression protocol was maintained for 3 weeks and consisted of three cycles of 50 mg cyclophosphamide/kg body weight for 4 consecutive days, with an interval of 3 days between each cycle.[33] Parasitemia at that stage was evaluated from the next day after finishing the third cycle, according to the procedure described for the acute phase. After that, the animals were sacrified. Animals were considered cured when, after inoculation with *T. cruzi* and further treatment with the testing compounds, reappearance of parasitemia after three cycles of immunosuppression was not found[51] and/or the presence of amastigote nests or other forms of parasites in histological sections was not observed.

ELISA.[34] Fe-SOD excreted from the parasite, cultured and processed as described in the corresponding section, was used as the antigen fraction. The total homogenate and purified protein fractions were coated onto polystyrene microtiter plates (Nunc, Denmark) at 5 and 1.5 μg, respectively, in carbonate buffer (pH 8.2) for 2 h at 37 °C. The antigen remaining on the plate was eliminated by washing three

times with 0.05% PBS-Tween 20 (washing buffer). Free adsorption sites were taken by incubation (2 h at 37 °C) with blocking buffer [0.2% PBS-Tween 20, 1% bovine serum albumin (BSA)]. After the the mixture was washed as described previously, the plates were incubated (45 min at 37 °C) with a serum dilution of 1:100 in washing buffer. After a second wash, the plates were incubated in darkness for 20 min with 100 μL of an enzyme-conjugated antibody (anti-IgG peroxidase) at a dilution of 1:1000. The enzyme reaction was developed with the chromogenic substrate *o*-phenylenediamine dihydrochloride (OPD, Sigma) and 10 μL of 30% H_2O_2 per 25 mL for 20 min in the dark. The reaction was stopped by the addition of 50 μL of HCl, 3 N. Absorbance was read at 492 nm in a microplate reader (Sunrise, TECAN). All of the samples were analyzed in triplicate in polystyrene microtiter plates. Mean and standard deviations of the optical densities of the negative control sera were used to calculate the cutoff value.

Metabolite Excretion. Cultures of *T. cruzi* epimastigotes (initial concentration of 5×10^5 cells/mL) received IC_{25} of the compounds (except for the control cultures). After incubation for 96 h at 28 °C, the cells were centrifuged at 400*g* for 10 min. The supernatants were collected in order to determine the excreted metabolites through ^1H NMR, and the chemical shifts were expressed in parts per million (ppm), using sodium 2,2-dimethyl-2-silapentane-5-sulfonate as the reference signal. The chemical displacements used to identify the respective metabolites were consistent with those described previously by us.[52]

Ultrastructural Alterations. The parasites were cultured at a density of 5×10^5 cells/mL in each corresponding medium containing the compounds tested at the concentration of IC_{25}. After 96 h, these cultures were centrifuged at 400*g* for 10 min, and the pellets produced were washed in PBS before being then mixed with 2% (v/v) paraformaldehyde/glutaraldehyde in 0.05 M cacodylate buffer (pH 7.4) for 4 h at 4 °C. Following this, the pellets were prepared for transmission electron microscopy study using a technique described by us.[53]

■ ASSOCIATED CONTENT

Supporting Information

Results from combustion analysis, molecular modeling of interactions with the Fe-SOD enzyme, and NMR spectra obtained from the metabolite excretion studies. This material is available free of charge via the Internet at http://pubs.acs.org.

■ AUTHOR INFORMATION

Corresponding Author

*For M.S.-M.: phone, +34-958-242-369; fax, +34-958-243-862; e-mail, msanchem@ugr.es. For F.G.-C.: phone, +34-91-394-4229; fax, +34-91-394-4103; e-mail, fercon@quim.ucm.es. For P.N.: phone, +34-91-258-7572; fax, +34-91-564-4853; e-mail, iqmnt38@iqm.csic.es.

Notes

Conflict of Interest Disclosure. The authors declare no competing financial interest.

■ ACKNOWLEDGMENTS

The authors thank the MCINN Projects: Consolider Ingenio CSD2010-00065 and CTQ2009-14288-C04-01 for financial support. We are also grateful to the NMR and elemental analysis by CAI of the Universidad Complutense (Madrid, Spain) and also to the transmission electron microscopy and nuclear magnetic resonance spectroscopy services of the CIC-University of Granada, Spain.

■ DEDICATION

This paper is dedicated to the memory of Prof. Mercedes Pardo Criado, without whose contribution and enthusiasm the synthetic branch of this research group would not have evolved as it has. She is sorely missed.

■ ABBREVIATIONS USED

SOD, superoxide dismutase; BZN, benznidazole; NADH, nicotinamide adenine dinucleotide; AIDS, acquired immunodeficiency syndrome; TEM, transmission electron microscopy; HMQC, heteronuclear single quantum coherence experiment; SI, selectivity index; dpi, days postinfection; IgG, immunoglobulin G; ELISA, enzyme-linked immunosorbent assay; OD, optical density; SD, standard deviation; PEP, phosphoenolpyruvate; TLC, thin-layer chromatography; HMBC, heteronuclear multiple-bond correlation spectroscopy; TMS, tetramethylsilane; DMSO, dimethylsulfoxide; MS-ESI, electrospray ionization mass spectrometry; FBS, fetal bovine serum; RPMI, Roswell Park Memorial Institute; MES, 4-morpholinoethanesulfonic acid; PBS, phosphate buffered saline solution; FCS, fetal calf serum; MTL, medium trypanosomes liquid; EDTA, ethylendiaminetetraacetic acid; STE, sodium chloride−Tris−EDTA; NBT, nitroblue tetrazolium; BSA, bovine serum albumin; OPD, *o*-phenylenediamine dihydrochloride

■ REFERENCES

(1) Mc Kerrow, J. H.; Doyle, P. S.; Engel, J. C.; Podust, L. M.; Robertson, S. A.; Ferreira, R.; Saxton, T.; Arkin, M.; Kerr, I. D.; Brinen, I. S.; Craik, C. S. Two approaches to discovering and developing new drugs for Chagas disease. *Mem. Inst. Oswaldo Cruz* **2009**, *104*, 263−269.

(2) Rassi, A., Jr.; Rassi, A.; Marin-Neto, J. A. Chagas disease. *Lancet* **2010**, *375*, 1388−1402.

(3) Gascon, J.; Bern, C.; Pinazo, M. J. Chagas disease in Spain, the United States and other non-endemic countries. *Acta Trop.* **2010**, *115*, 22−27.

(4) Bern, C.; Montgomery, S. P.; Katz, L.; Caglioti, S.; Stramer, S. L. Chagas disease and the US blood supply. *Curr. Opin. Infect. Dis.* **2008**, *21*, 476−482.

(5) Apt, W.; Zulantay, I. Estado actual en el tratamiento de la enfermedad de Chagas. *Rev. Med. Chile* **2011**, *139*, 247−257.

(6) Hall, B. S.; Wilkinson, S. R. Activation of benznidazole by trypanosomal type I nitroreductases results in glyoxal formation. *Antimicrob. Agents Chemother.* **2012**, *56* (1), 115−123.

(7) Viotti, R.; Vigliano, C.; Lococo, B.; Alvarez, M. G.; Petti, M.; Bertocchi, G.; Armenti, A. Side-effects of benznidazole as treatment in chronic Chagas disease: fears and realities. *Expert Rev. Anti-Infect. Ther.* **2009**, *7*, 157−163.

(8) Castro, J. A.; de Mecca, J. J.; Bartel, L. C. Toxic side effects of drugs used to treat Chagas disease. *Hum. Exp. Toxicol.* **2006**, *25* (8), 471−479.

(9) Coura, J. R.; de Castro, S. L. A critical review on Chagas disease chemotherapy. *Mem. Inst. Oswaldo Cruz* **2002**, *97*, 3−24.

(10) Le Loup, G.; Ibrahim, K.; Malvy, D. Chagas disease and immunodeficiency: HIV infection and transplantation. *Bull. Soc. Pathol. Exot.* **2009**, *102* (5), 310−318.

(11) Rivera, J.; Hillis, L. D.; Levine, B. D. Reactivation of cardiac Chagas disease in acquired immune deficiency syndrome. *Am. J. Cardiol.* **2004**, *94*, 1102−1103.

(12) Gallerano, V.; Consigli, J.; Pereyra, S.; Gomez-Zanni, S.; Danielo, C.; Gallerano, R. H.; Guidi, A. Chagas disease reactivation with skin symptoms in a patient with kidney transplant. *Int. J. Dermatol.* **2007**, *46*, 607−610.

(13) Center for Disease Control and Prevention. Chagas disease after organ transplantation. *Morbidity Mortality Wkly. Rep.* **2001**, *51*, 210−212.

(14) Corti, M.; Yampolski, C. Prolonged survival and immune reconstitution ater chagasic meningoencephalitis in a patient with

acquired immunodeficiency syndrome. *Rev. Soc. Bras. Med. Trop.* **2006**, *39*, 85−88.
(15) Ferreira, M. S. Chagas disease and immunosuppression. *Mem Inst. Oswaldo Cruz* **1999**, *94*, 325−327.
(16) Campos, S. V.; Strabelli, T. M. V.; Neto, V. A.; Silva, C. P.; Bacal, F.; Bocchi, E. A.; Stolf, N. A. G. Risk factors for Chagas disease reactivation after heart transplantation. *J. Heart Lung Transplant.* **2008**, *27* (6), 597−602.
(17) Doyle, P. S.; Zhou, Y. M.; Engel, J. M.; McKerrow, J. H. A cysteine protease inhibitor cures Chagas disease in an immunodeficient-mouse model of infection. *Antimicrob. Agents Chemother.* **2007**, *51* (11), 3932−3939.
(18) Soeiro, M. N.; de Castro, S. L. *Trypanosoma cruzi* targets for new chemotherapeutic approaches. *Expert Opin. Ther. Targets* **2009**, *13* (1), 105−121.
(19) (a) Mehlotra, R. K. Antioxidant defense mechanisms in parasitic protozoa. *Crit. Rev. Microbiol.* **1996**, *22* (4), 295−314. (b) Atwood, J. A., 3rd; Weatherly, D. B.; Minning, T. A.; Bundy, B.; Cavola, C.; Opperdoes, F. R.; Orlando, R.; Tarleton, R. L. The *Trypanosoma cruzi* proteome. *Science* **2005**, *309*, 473−476.
(20) Rodriguez-Ciria, M.; Sanz, A. M.; Yunta, M. J. R.; Gomez-Contreras, F.; Navarro, P.; Sanchez-Moreno, M.; Booutaleb-Charki, S.; Osuna, A.; Castiñeiras, A.; Pardo, M.; Cano, C.; Campayo, L. 1,4-Bis(alkylamino)benzo[*g*]phthalazines able to form complexes of Cu(II) which as free ligands behave as SOD inhibitors and show efficient in vitro activity against *Trypanosoma cruzi*. *Bioorg. Med. Chem.* **2007**, *15*, 2081−2091.
(21) Sanz, A. M.; Gomez-Contreras, F.; Navarro, P.; Sánchez-Moreno, M.; Boutaleb-Charki, S.; Campuzano, J.; Pardo, M.; Osuna, A.; Cano, C.; Yunta, M. J. R.; Campayo, L. Efficient inhibition of Fe-SOD and of *Trypanosoma cruzi* growth by benzo[*g*]phthalazine derivatives functionalized with one or two imidazole rings. *J. Med. Chem.* **2008**, *51*, 1962−1966.
(22) Sánchez-Moreno, M.; Sanz, A. M.; Gómez-Contreras, F.; Navarro, P.; Marín, C.; Ramírez-Macias, I.; Rosales, M. J.; Olmo, F.; Garcia-Aranda, I.; Campayo, L.; Cano, C.; Arrebola, F.; Yunta, M. J. R. In vivo trypanosomicidal activity of imidazole- or pyrazole-based benzo[*g*]phthalazine derivatives against acute and chronic phases of Chagas disease. *J. Med. Chem.* **2011**, *54*, 970−979.
(23) Sánchez-Moreno, M.; Gómez-Contreras, F.; Navarro, P.; Marín, C.; Ramírez-Macías, I.; Olmo, F.; Sanz, A. M.; Campayo, L.; Cano, C.; Yunta, M. J. R. In vitro leishmanicidal activity of imidazole- or pyrazole-based benzo[*g*]phthalazine derivatives against *L. infantum* and *L. braziliensis* species. *J. Antimicrob. Chemother.* **2012**, *67*, 387−397.
(24) López-Antuñano, F. J. Quimioterapia de las infecciones producidas por *Trypanosoma cruzi*. *Salud Publica Mex.* **1997**, *39* (5), 463−471.
(25) Sánchez-Moreno, M.; Marín, C.; Navarro, P.; Lamarque, L.; García-España, E.; Miranda, C.; Huertas, O.; Olmo, F.; Gómez-Contreras, F.; Pitarch, J.; Arrebola., F. In vitro and in vivo trypanosomicidal activity of pyrazole-containing macrocyclic and macrobicyclic polyamines: their action on acute and chronic phases of Chagas disease. *J. Med. Chem.* **2012**, *55* (9), 4231−4243.
(26) Villagran, M. E.; Marin, C.; Rodriguez-González, I.; de Diego, J. A.; Sanchez-Moreno, M. Use of an iron superoxide dismutase excreted by *T. cruzi* in the diagnosis of Chagas disease: seroprevalence in rural zones of the state of Queretaro, Mexico. *Am. J. Trop. Med. Hyg.* **2005**, *73*, 510−516.
(27) Miller, A. F.; Sorkin, D. L.; Padmakumar, K. Anion binding properties of reduced and oxidized iron-containing superoxide dismutase reveal no requirement for tyrosine 34. *Biochemistry* **2005**, *44*, 5969−5981.
(28) Yikilmaz, E.; Rodgers, D. W.; Miller, A. F. The crucial importance of chemistry in the structure−function link: manipulating hydrogen bonding in iron-containing superoxide dismutase. *Biochemistry* **2006**, *45*, 1151−1161.
(29) (a) Vance, C. K.; Miller, A. F. Specificity and phenetic relationships of iron- and manganese-containing superoxide dismutases on the basis of structure and sequence comparisons. *Biochemistry* **2001**, *40*, 13079−13087. (b) Yikilmaz, E.; Xie, J.; Brunold, T. C.; Miller, A. F. Hydrogen-bond-mediated tuning of the redox potential of the non-heme Fe site of superoxide dismutase. *J. Am. Chem. Soc.* **2002**, *124*, 3482−3483. (c) Vance, C. K.; Miller, A.-F. A simple proposal that can explain the inactivity of metal-substituted superoxide dismutases. *J. Am. Chem. Soc.* **1998**, *120*, 461−467. (d) Stallings, W. C.; Metzger, A. L.; Pattridge, K. A.; Fee, J. A.; Ludwig, M. L. Structure−function relationships in iron and manganese superoxide dismutases. *Free Radical Res. Commun.* **1991**, *12*−*13*, 259−268.
(30) Han, W. G.; Lovell, T.; Noodleman, L. Coupled redox potentials in manganese and iron superoxide dismutases from reaction kinetics and density functional/electrostatics calculations. *Inorg. Chem.* **2002**, *41*, 205−218.
(31) Muñoz, I. G.; Moran, J. F.; Becana, M.; Montoya, G. The crystal structure of a eukaryotic iron superoxide dismutase suggests intersubunit cooperation during catalysis. *Protein Sci.* **2005**, *14*, 387−394.
(32) Da Silva, C. F.; Batista, M. M.; Batista, D. G. J.; de Souza, E. M.; da Silva, P. B.; de Oliveira, G. M.; Meuser, A. S.; Shareef, A. R.; Boykin, D. W.; Soeiro, M. N. C. In vitro and in vivo studies of the trypanocidal activity of a diarylthiophene diamidine against *Trypanosoma cruzi*. *Antimicrob. Agents Chemother.* **2008**, *9*, 3307−3314.
(33) Caldas, S; Santos, F. M.; de Lana, M.; Diniz, L. F.; Machado-Coelho, G. L.; Veloso, V. M.; Bahia, M. T. *Trypanosoma cruzi*: acute and long-term infection in the vertebrate host can modify the response to benznidazole. *Exp. Parasitol.* **2008**, *118* (3), 315−323.
(34) Lopez-Cespedes, A.; Villagran, E.; Briceño-Alvarez, K.; de Diego, J. A.; Hernandez-Montiel, H. L.; Saldaña, C.; Sanchez-Moreno, M.; Marin, C. *Trypanosoma cruzi*: seroprevalence detection in suburban population of Santiago de Queretaro(Mexico). *Sci. World J.* **2012**, DOI: 10.1100/2012/914129.
(35) El Bouhdidi, A.; Truyens, C.; Rivera, M. T.; Bazin, H.; Carlier, Y. *Trypanosoma cruzi* infection in mice induces a polyisotopic hypergammaglobulinemia and parasite-specific response involving high IgG2a concentrations and highly avid IgG1 antibodies. *Parasite Immunol.* **1994**, *16* (2), 69−76.
(36) Ginger, M. Trypanosomatid biology and euglenozoan evolution: new insights and shifting paradigms revealed through genome sequencing. *Protist* **2005**, *156* (4), 377−392.
(37) Cazzulo, J. J. Aerobic fermentation of glucose by trypanosomatids. *FASEB J.* **1992**, *6* (13), 3153−3161.
(38) Costou, V.; Besteiro, S.; Riviere, L.; Biran, M.; Biteau, N.; Franconi, J. M.; Boshart, M.; Baltz, T.; Bringaud, F. A mitochondrial NADH-dependent fumarate reductase involved in the production of succinate excreted by procyclic *Trypanosoma brucei*. *J. Biol. Chem.* **2005**, *280* (17), 16559−16570.
(39) Bringaud, F.; Riviere, L.; Coustou, V. Energy metabolism of trypanosomatids: adaptation to available carbon sources. *Mol. Biochem. Parasitol.* **2006**, *149*, 1−9.
(40) Hirsch, A.; Orphanos, D. Quantitative preparation of chloro- and bromophthalazines. *Can. J. Chem.* **1965**, *43*, 2708−2710.
(41) Perrin, D. D.; Armarego, W. L. F.; Perrin, D. R. *Purification of Laboratory Chemicals*; Pergamon Press: Oxford, U.K., 1980.
(42) Téllez-Meneses, J.; Mejía-Jaramillo, A. M.; Triana-Chávez, O. Biological characterization of *Trypanosoma cruzi* stocks from domestic and sylvatic vectors in Sierra Nevada of Santa Marta, Colombia. *Acta Trop.* **2008**, *108*, 26−34.
(43) Osuna, A.; Adroher, F. J.; Lupiañez, J. A. Influence of electrolytes and non-electrolytes on growth and differentiation of Trypanosoma cruzi. *Cell Differ. Dev.* **1990**, *30*, 89−95.
(44) Marín, C.; Ramírez-Macías, I.; López-Céspedes, A.; Olmo, F.; Villegas, N.; Díaz, J. G.; Rosales, M. J.; Gutierrez-Sánchez, R.; Sánchez-Moreno, M. In vitro and in vivo trypanocidal activity of flavonoids from *Delphinium staphisagria* against Chagas disease. *J. Nat. Prod.* **2011**, *74*, 744−750.
(45) Moreno, D.; Plano, D.; Baquedano, Y.; Jiménez-Ruiz, A.; Palop, J. A.; Sanmartín, C. Antileishmanial activity of imidothiocarbamates and imidoselenocarbamates. *Parasitol. Res.* **2011**, *108*, 233−239.

(46) González, P.; Marín, C.; Rodríguez-González, I.; Hitos, A. B.; Rosales, M. J.; Reina, M.; Díaz, J. G.; Gonzalez-Coloma, A.; Sanchez-Moreno, M. In vitro activity of C_{20}-diterpenoid alkaloid derivatives in promastigotes and intracellular amastigotes of *Leishmania infantum*. *Int. J. Antimicrob. Agents* **2005**, *25*, 136−141.
(47) Bradford, M. M. A refined and sensitive method for the quantification of microquantities of protein−dye binding. *Anal. Biochem.* **1976**, *72*, 248−252.
(48) Beyer, W. F.; Fridovich, I. Assaying for superoxide dismutase activity: some large consequences of minor changes in conditions. *Anal. Biochem.* **1987**, *161*, 559−566.
(49) *HyperChem Professional 8.0*; Hypercube, Inc. (1115 NW 4th Street, Gainesville, FL 32601, U.S.).
(50) Miranda, C.; Escartí, F.; Lamarque, L.; Yunta, M. J. R.; Navarro, P.; García-España, E.; Jimeno, M. L. New 1*H*-pyrazole-containing polyamine receptors able to complex L-glutamate in water at physiological pH values. *J. Am. Chem. Soc.* **2004**, *126*, 823−833.
(51) Santos, D. M.; Martins, T. A. F.; Caldas, I. S.; Diniz, L. F.; Machado-Coelho, G. L. L.; Carneiro, C. M.; Oliveira, R. P.; Talvani, A.; Lana, M.; Bahia, M. T. Benznidazole alters the pattern of cyclophosphamide-induced reactivation in experimental *Trypanosoma cruzi*-dependent linage infection. *Acta Trop.* **2010**, *113* (2), 134−138.
(52) Fernandez-Becerra, C.; Sánchez-Moreno, M.; Osuna, A.; Opperdoes, F. R. Comparative aspects of energy metabolism in plant trypanosomatids. *J. Eukaryotic Microbiol.* **1997**, *44* (5), 523−529.
(53) González, P.; Marín, C.; Rodríguez-González, I.; Hitos, A. B.; Rosales, M. J.; Reina, M.; Díaz, J. G.; Gonzalez-Coloma, A.; Sanchez-Moreno, M. In vitro activity of C_{20}-diterpenoid alkaloid derivatives in promastigotes and intracellular amastigotes of *Leishmania infantum*. *Int. J. Antimicrob. Agents* **2005**, *25*, 136−141.